Progress In Electromagnetics Research, *PIER 12, 277–302, 1996*

ASYMPTOTIC EXPANSIONS FOR GREEN'S DYADICS IN BIANISOTROPIC MEDIA

B. Jakoby and F. Olyslager

1. Introduction

Complex linear media have been studied for some time now including special cases such as optically active (chiral) media at optical frequencies or magnetoelectric media at quasistatic conditions. Recently generally bianisotropic media again received increasing importance in electromagnetic theory due to advances in material science which enable the manufacturing of more complex composite media acting as bianisotropic materials at microwave frequencies [1]. Apart from the general bianisotropic case, several special cases have been investigated in order to derive closed form results yielding additional insight compared to numerical methods. The constitutive equations for general bianisotropic media read [2]

$$\mathbf{D} = \underline{\underline{\varepsilon}} \cdot \mathbf{E} + \underline{\underline{\xi}} \cdot \mathbf{H} \tag{1a}$$

$$\mathbf{B} = \underline{\underline{\zeta}} \cdot \mathbf{E} + \underline{\underline{\mu}} \cdot \mathbf{H} \tag{1b}$$

Special interests have been devoted to the determination of closed form Green's dyadics in homogeneous bianisotropic media. Here the complexity of the solution increases fast with the number of free parameters in the material tensors $\underline{\underline{\varepsilon}}, \underline{\underline{\mu}}, \underline{\underline{\xi}}$, and $\underline{\underline{\zeta}}$. Up to now, the number of parameters which allow closed form representations of Green's dyadics is rather limited. See [3] and [4] for some recent advances and [5] for a clear overview on existing closed form solutions.

It hence appears as if the complexity enabling the derivation of closed form Green's functions has been reached. In this paper we derive a closed form Green's dyadic for the electric field in the *spectral* domain by utilizing a three-dimensional Fourier transform. In principle, similar approaches have been proposed considerable time ago [6] for special kinds of anisotropic media. A decomposition of the spectral representation allows the evaluation of the asymptotic behavior in spatial domain in the far field as well as close to the source point. In this work, we discuss an approach for general, bianisotropic media yielding a complete and reduced integral representation of the solution together with asymptotic approximations.

The applicability of the method is demonstrated by considering a diagonally or biaxial bianisotropic medium leading to comparably simple expressions.

2. Theory

Considering Maxwell's curl equations for the fields in the presence of an impressed electric current density distribution $\mathbf{J}$ (time dependence $\exp(j\omega t)$ is assumed)

$$\nabla \times \mathbf{H}(\mathbf{r}, \omega) = \mathbf{J}(\mathbf{r}, \omega) + j\omega \mathbf{D}(\mathbf{r}, \omega) \tag{2a}$$

$$\nabla \times \mathbf{E}(\mathbf{r}, \omega) = -j\omega \mathbf{B}(\mathbf{r}, \omega) \tag{2b}$$

together with the constitutive equations (1) allows the derivation of the following differential equation for the electric field vector [7]

$$\underline{\underline{\mathcal{H}}}(\nabla, \underline{\underline{\varepsilon}}, \underline{\underline{\mu}}, \underline{\underline{\xi}}, \underline{\underline{\zeta}}, \omega) \cdot \mathbf{E} = -j\omega \mathbf{J} \tag{3}$$

where

$$\underline{\underline{\mathcal{H}}}(\nabla, \underline{\underline{\varepsilon}}, \underline{\underline{\mu}}, \underline{\underline{\xi}}, \underline{\underline{\zeta}}, \omega) = (\nabla \times \underline{\underline{\mathbf{I}}} - j\omega \underline{\underline{\xi}}) \cdot \underline{\underline{\mu}}^{-1} \cdot (\nabla \times \underline{\underline{\mathbf{I}}} + j\omega \underline{\underline{\zeta}}) - \omega^2 \underline{\underline{\varepsilon}} \tag{4}$$

In the bi-isotropic case, the operator on the left hand side can be factorized into two (commuting) operators of the principal form

$$\underline{\underline{\mathcal{H}}}_{\pm} = (\nabla \times \underline{\underline{\mathbf{I}}} \mp k_{\pm}), \tag{5}$$

describing circularly polarized eigenstates [7]. However, in the general bianisotropic case this is not possible. If we subject the spatial rectangular co-ordinates to a Fourier transform according to

$$\mathbf{F}(x,y,z) = \int\int\int \frac{d^3k}{(2\pi)^3}\ \widetilde{\mathbf{F}}(k_x,k_y,k_z)\ \mathrm{e}^{-j\mathbf{k}\cdot\mathbf{r}} \tag{6}$$

where $\mathbf{r} = [x,y,z]^T$, $\mathbf{k} = [k_x,k_y,k_z]^T$ (the superscript T denotes transposition), we arrive at an algebraic matrix equation:

$$\widetilde{\underline{\underline{\mathcal{H}}}} \cdot \widetilde{\mathbf{E}} = -j\omega\widetilde{\mathbf{J}} \tag{7}$$

The matrix $\widetilde{\underline{\underline{\mathcal{H}}}}$ represents the operator $\underline{\underline{\mathcal{H}}}$ in the spectral (wavenumber) domain in which the spatial derivatives transform according to $\partial/\partial\nu \leftrightarrow -jk_\nu$ $(\nu = x,y,z)$. In the source free case, (7) represents a homogeneous matrix equation that leads to non-trivial solutions only if its determinant vanishes

$$F(k_x,k_y,k_z,\omega) = \det\left[\widetilde{\underline{\underline{\mathcal{H}}}}(k_x,k_y,k_z,\omega)\right] = 0 \tag{8}$$

Equation (8) is the dispersion relation for plane waves in a homogeneous medium. It can be seen by considering Maxwell's equations in the wavenumber domain, that explicit frequency appearance in the dispersion relation can be avoided by substituting wavenumbers by the so-called slownesses

$$s_\nu = \frac{k_\nu}{\omega} \quad (\nu = x,y,z) \tag{9}$$

that, for real valued wavenumbers, equal the inverse of the phase velocity component in the direction ν. For lossless media, the dispersion relation (8) describes algebraic surfaces of fourth order in the real wavenumber space at frequency ω. The shape of these so-called wavenumber surfaces determines the direction of the group velocity $\mathbf{v}_g$, which is oriented normal to the wavenumber surface in the point corresponding to the plane wave under consideration [8,9]:

$$\mathbf{v}_g = \nabla_k\ \omega = -\frac{\nabla_k\ F}{\dfrac{dF}{d\omega}} \tag{10}$$

Here ∇_k denotes the gradient in the $\mathbf{k}$ domain. The denominator represents the total derivative of F with respect to ω and thus includes the effects of dispersion due to frequency dependent material parameters as well. The latter, however, is often neglected such that the total derivative reduces to a partial derivative of F with respect to ω. The coefficients of the polynomial $\det\left[\underline{\underline{\widetilde{\mathcal{H}}}}(k_x, k_y, k_z, \omega)\right]$ have been classified in [10]. In addition we note, that for reciprocal media wavenumber surfaces are point symmetric with respect to the origin: if (k_x, k_y, k_z) is a point on a wavenumber surface, then $(-k_x, -k_y, -k_z)$ is also one. A bianisotropic medium is reciprocal if [2]

$$\underline{\underline{\varepsilon}} = \underline{\underline{\varepsilon}}^T, \; \underline{\underline{\mu}} = \underline{\underline{\mu}}^T, \; \underline{\underline{\xi}} = -\underline{\underline{\zeta}}^T \tag{11}$$

For a given current distribution $\mathbf{J}$ the spectral fields can be readily expressed in the spectral domain

$$\widetilde{\mathbf{E}} = -j\omega \underline{\underline{\widetilde{\mathcal{H}}}}^{-1} \cdot \widetilde{\mathbf{J}} \tag{12}$$

which means that the spectral Green's dyadic for the electric field is given by

$$\underline{\underline{\widetilde{\mathcal{G}}}}_{ee} = -j\omega \underline{\underline{\widetilde{\mathcal{H}}}}^{-1} \tag{13}$$

where the subscript ee indicates that we are considering electric fields due to an electric dipole. We will restrict ourselves to $\underline{\underline{\widetilde{\mathcal{G}}}}_{ee}$ since $\underline{\underline{\widetilde{\mathcal{G}}}}_{me}$ (magnetic fields due to electric dipoles) can be derived from $\underline{\underline{\widetilde{\mathcal{G}}}}_{ee}$ by simple algebraic manipulations [7] and the dyadics for magnetic sources, $\underline{\underline{\widetilde{\mathcal{G}}}}_{em}$ and $\underline{\underline{\widetilde{\mathcal{G}}}}_{mm}$, can be obtained by using the duality principle. The approach outlined in the sequel is applicable to each of these dyadics.

The inverse of $\underline{\underline{\mathcal{H}}}$ can be written as

$$\underline{\underline{\widetilde{\mathcal{H}}}}^{-1} = \frac{\underline{\underline{\widetilde{\mathcal{H}}}}^{adj}}{\det(\underline{\underline{\widetilde{\mathcal{H}}}})} = \frac{\underline{\underline{\widetilde{\mathcal{H}}}}^{adj}}{F} \tag{14}$$

where $\underline{\underline{\widetilde{\mathcal{H}}}}^{adj}$ is the adjoint matrix of $\underline{\underline{\widetilde{\mathcal{H}}}}$. The elements of $\underline{\underline{\widetilde{\mathcal{H}}}}^{adj}$ are polynomials in the wavenumber components. The denominator contains the polynomial determining the dispersion relation (8), which leads to pole singularities in spectral Green's dyadics at all wavenumber triplets (k_x, k_y, k_z) representing solutions of the dispersion equation at the considered frequency and which hence correspond to points on a wavenumber surface. We note that at isolated points, denominator zeros can be canceled by zeros in the numerator, which means that the respective wave is not excited by the source associated with the Green's function under consideration.

The residues of these poles prescribe the amplitudes of the launched plane waves, that, in turn, determine the asymptotic far field behavior in spatial domain. Let us examine this issue more in detail.

It is more convenient to treat the problem in spherical co-ordinates in spatial domain

$$x = r\sin\theta\cos\phi,\ \ y = r\sin\theta\sin\phi,\ \ z = r\cos\theta \tag{15}$$

while in the spectral domain we shall use spherical co-ordinates k, ϑ, φ with respect to a rotated frame, whose $k_{z'}$ axis is parallel to the vector $\mathbf{r}$ pointing from the source to the observation point:

$$k_{x'} = k\sin\vartheta\cos\varphi,\ \ k_{y'} = k\sin\vartheta\sin\varphi,\ \ k_{z'} = k\cos\vartheta \tag{16}$$

The $k_{x'}$ axis of the rotated frame is chosen to lie in the x, y plane of the original frame (see Fig. 1).

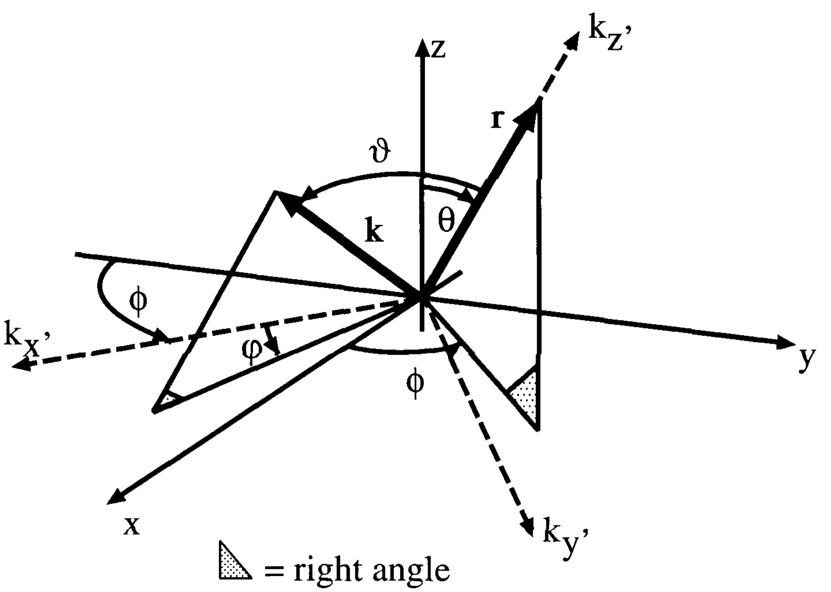

Figure 1. The rotated co-ordinate system (rotated axes are given as dashed lines). The x' axis lies in the x, y plane; the angles φ, ϑ are spherical angles in the rotated system.

For the sake of notational simplicity, ω will frequently be omitted from the argument lists in the following since we are considering time harmonic fields at a given, constant frequency. The inverse transform can then be written as

$$\underline{\underline{\mathcal{G}}}_{ee}(r,\phi,\theta) = \frac{1}{(2\pi)^3} \int\int\limits_{K^3}\int d\vartheta\ d\varphi\ dk\ k^2\ \sin\vartheta\ \underline{\underline{\widetilde{\mathcal{G}}}}_{ee}(k,\varphi,\vartheta)\ \mathrm{e}^{-jkr\cos\vartheta} \tag{17}$$

where ϑ denotes the angle between $\mathbf{k}$ and $\mathbf{r}$ according to the co-ordinate frame chosen for k,ϑ,φ. Below we will use two different sets of integration ranges for the co-ordinates k,φ and ϑ covering the entire wavenumber domain K^3, thus we do not specify them explicitly at the moment.

As outlined above, $\underline{\underline{\widetilde{\mathcal{G}}}}_{ee}$ features poles at points belonging to wavenumber surfaces. In spherical co-ordinates the solutions of the dispersion equation can be written as

$$k = k_{1,2,3,4}(\varphi,\vartheta,\omega) \tag{18}$$

Commonly, these solutions can be considered as two pairs belonging to the same wavenumber surface each. Due to the aforementioned symmetry in case of reciprocal media we can assign pairs (k_1,k_3) and (k_2,k_4) where

$$k_1(\varphi,\vartheta,\omega) = -k_3(\varphi,\vartheta,\omega),\ \ k_2(\varphi,\vartheta,\omega) = -k_4(\varphi,\vartheta,\omega) \tag{19}$$

(reciprocal media)

For given φ and ϑ the integrand of (17) represents a rational function in k with four poles at $k_{1,2,3,4}$. Furthermore we have a double pole at infinity which is essentially introduced by the k^2 of the Jacobian. The integrand may be decomposed using a partial fraction expansion for the part being rational in k:

$$k^2\ \underline{\underline{\widetilde{\mathcal{G}}}}_{ee}(k,\varphi,\vartheta) = \sum_{i=1}^{4} \frac{\underline{\underline{\mathbf{A}}}_i(\varphi,\vartheta)}{k-k_i(\varphi,\vartheta)} + \underline{\underline{\mathbf{B}}}(\varphi,\vartheta) + \underline{\underline{\mathbf{C}}}(\varphi,\vartheta)\ k + \underline{\underline{\mathbf{D}}}(\varphi,\vartheta)\ k^2 \tag{20}$$

The elements of $\underline{\underline{\mathbf{A}}}_i$ can be expressed in terms of the residues of the Green's function

$$\underline{\underline{\mathbf{A}}}_i = k_i^2\ \mathrm{Res}_{k_i}\left\{\underline{\underline{\widetilde{\mathcal{G}}}}_{ee}\right\} \tag{21}$$

while we have for

$$\underline{\underline{\mathbf{D}}} = \lim_{k\to\infty} \underline{\underline{\widetilde{\mathcal{G}}}}_{ee} \tag{22}$$

$$\underline{\underline{\mathbf{C}}} = \lim_{k\to\infty} \left[k(\underline{\underline{\widetilde{\mathcal{G}}}}_{ee} - \underline{\underline{\mathbf{D}}}) \right] \tag{23}$$

$$\underline{\underline{\mathbf{B}}} = \lim_{k\to\infty} \left[k^2(\underline{\underline{\widetilde{\mathcal{G}}}}_{ee} - \underline{\underline{\mathbf{D}}}) - k\underline{\underline{\mathbf{C}}} \right] \tag{24}$$

In case of multiple roots, the Green's dyadic still shows first order poles only, since one pole is canceled by a zero in the numerator as it is shown in Appendix B. The sum runs over less than four first order poles in this case.

For reciprocal media, the Green's dyadic $\underline{\underline{\widetilde{\mathcal{G}}}}_{ee}$ fulfills [8,11]

$$\underline{\underline{\widetilde{\mathcal{G}}}}_{ee}(\mathbf{k}) = \underline{\underline{\widetilde{\mathcal{G}}}}_{ee}^{T}(-\mathbf{k}) \tag{25}$$

which, using (19), leads to

$$A_{ij,1} = -A_{ji,3}, \; A_{ij,2} = -A_{ji,4} \tag{26}$$

$$B_{ij} = B_{ji} \tag{27}$$

$$C_{ij} = -C_{ji} \tag{28}$$

$$D_{ij} = D_{ji} \tag{29}$$

Of particular interest are the terms proportional to k^2 and $1/(k-k_i)$, that determine the asymptotic field behavior close to the dipole source and the far field behavior, respectively, as will be shown below.

The representation of the dyadics $\underline{\underline{\mathbf{A}}}$, $\underline{\underline{\mathbf{B}}}$, $\underline{\underline{\mathbf{C}}}$ and $\underline{\underline{\mathbf{D}}}$ in the rotated spherical co-ordinate system can be derived from their representation in the original system by simple substitutions given in Appendix A.

Let us consider the far field behavior first. The integral

$$\underline{\underline{\mathcal{G}}}^{a}_{ee}(r,\phi,\theta) = \frac{1}{(2\pi)^3} \int_0^{\pi/2} d\vartheta \, \sin\vartheta \int_0^{2\pi} d\varphi \int_{-\infty}^{\infty} dk \, \sum_{i=1}^{4} \frac{\underline{\underline{\mathbf{A}}}_i(\varphi,\vartheta)}{k-k_i(\varphi,\vartheta)} \, \mathrm{e}^{-jkr\cos\vartheta} \tag{30}$$

leads to an asymptotic approximation in the far field. Note that the integration ranges of k and ϑ in (17) differ from the commonly used ranges in order to facilitate easy application of the residue theorem below. With the chosen ranges, a solid angle of 2π is covered by varying the angular co-ordinate quantities, however, the introduction of negative values of the radial co-ordinate maintains that the integration covers the entire three-dimensional wavenumber domain. For the spatial co-ordinates we will assume the common ranges $r \in [0, \infty]$, $\phi \in [0, 2\pi]$, $\theta \in [0, \pi]$. Figure 2 shows a typical arrangement of the poles in the complex k-plane for fixed φ and ϑ. For 'common' lossless media we have typically two poles located on the positive and two on the negative k axis. The following analysis is not restricted to this case, however, we will consider the important case of lossless media which yields poles on the real k axis requiring the consideration of the radiation condition in order to determine the proper integration path. The generalization to the lossy case (featuring no poles on the real axis) is near at hand, though. To enable the application of Cauchy's theorem, the integration path has to be closed by an infinite semicircle in the upper or the lower halfplane depending on the sign of $r\cos\vartheta$ in the exponent. According to Jordan's Lemma [12] the semicircle then has to be closed in the lower half plane since in our case $r\cos\vartheta > 0$. The poles on the real axis require deformations of the integration path in order to fulfill the radiation condition which requires outward traveling waves. Figure 2 shows the typical path P which includes poles k_1 and k_2 and excludes k_3 and k_4 to satisfy the radiation condition as explained below. With this path we obtain

$$\underline{\underline{\mathcal{G}}}^{a}_{ee}(r,\phi,\theta) = -\frac{j}{(2\pi)^2}\int_0^{\pi/2} d\vartheta \sin\vartheta \int_0^{2\pi} d\varphi \sum_{i=1}^{2} \underline{\underline{\mathbf{A}}}_i(\varphi,\vartheta)\, \mathrm{e}^{-jk_i(\varphi,\vartheta) r\cos\vartheta} \tag{31}$$

This can be interpreted as an angular superposition of plane waves. The question whether a pole has to be included or excluded is decided upon considering the behavior of the related partial wave in the given spatial direction (ϕ, θ). Indeed the exponential $\exp(-jk_i(\varphi,\vartheta)\, r\cos\vartheta)$ *suggests* that the associated partial wave can be regarded as outward traveling wave if $k_i(\varphi,\vartheta) > 0$. But this is not the whole truth. Inspection of the phase yields information on the direction of the phase velocity only. The radiation condition, however, refers to the direction of energy transport which is associated with the group velocity [9]. For moderately anisotropic media these directions almost coincide, none the less the suggestion provided by the sign of k_i can be misleading especially for directions (φ, ϑ) that are almost normal to (ϕ, θ).

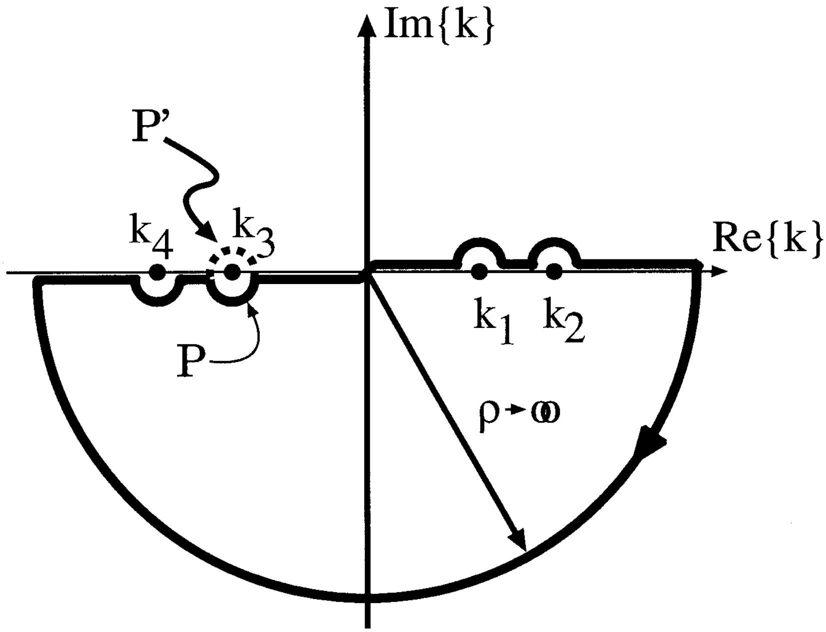

Figure 2. Integration contour for k-integration.

Figure 3 shows such a case in a 2D plot, which can be considered as a cut in the plane defined by the $\mathbf{r}$ and $\mathbf{k}$-vectors for fixed φ and ϑ. The shown curve represents the cut line between the (inner) wavenumber surface and the aforementioned plane. Thus the intersection points between k-axis and the curve correspond to k_1 and k_3 in Fig. 2. The related phase velocities oriented in parallel to the wave vectors actually show a component in the direction of $\mathbf{r}$ in case of k_1 and in the opposite direction for k_3. However, the group velocity, whose direction is determined by the normal vector on the wavenumber surface, features a component in the direction of $\mathbf{r}$ for both, k_1 as well as k_3. Hence both plane waves correspond to outward traveling waves with respect to direction (ϕ, θ) and thus have to be included in the integration contour as shown by the path P' in Fig. 2. We remark that the group velocity vectors do not necessarily lie in the sketched cut plane, their components in this plane are sufficient to determine their component with respect to $\mathbf{r}$, though. Of course it could also happen (and actually happens, e.g., in case of point symmetric wavenumber surfaces related to reciprocal media), that k_3 has to be included while k_1 has to be excluded at the same time. With these considerations, the sum $\sum_{i=1}^{2}$ in (31) should rather be interpreted as a sum over all i related partial waves with $\mathbf{v}_g \cdot \mathbf{r} > 0$.

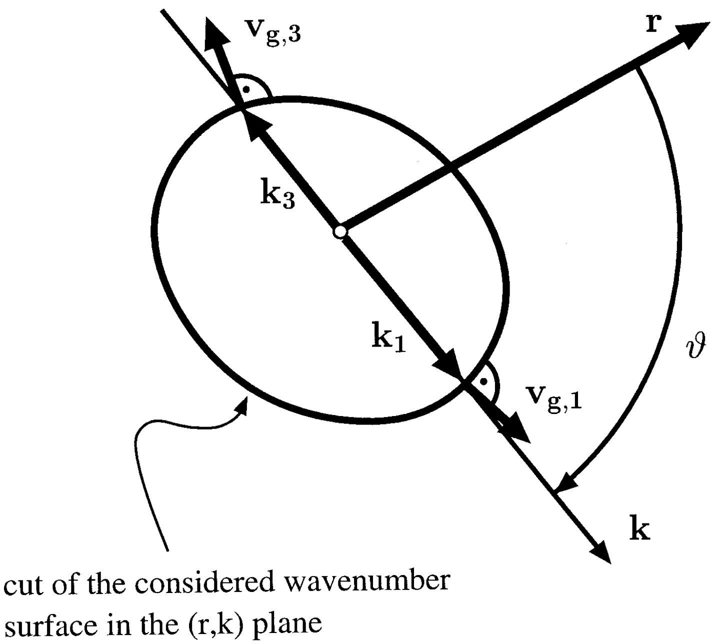

Figure 3. Checking the radiation condition for partial waves k_1 and k_3. In this (constructed) example, both partial waves at k_1 and k_2 feature $\mathbf{v}_g \cdot \mathbf{r} > 0$. The corresponding phase velocities are parallel to the wavevectors.

For sake of completeness, we mention that other definitions of the radiation condition for anisotropic media are used as well [13]. For instance, one can observe from which side the poles approach the real axis for vanishing losses in order to determine how to deform the integration path. These different approaches can lead to slightly different results. However, if the so obtained Green's functions are used in connection with Green's theorem for the treatment of problems involving finitely extended anisotropic regions, they lead to the same results for the fields. In that sense, the radiation condition simply acts as a condition ensuring a unique Green's function which has already pointed out by Okoshi [14], who investigated the application of Green's functions representing inward traveling waves for the analysis of closed regions. One can interpret this ambiguity as representation of the fact, that infinitely extended anisotropic regions do not exist. If, however, a problem includes the approximate model of an infinitely extended anisotropic region, one has to decide carefully upon which radiation condition has to be chosen.

$\underline{\underline{\mathcal{G}}}^a_{ee}(r,\phi,\theta)$ represents that part of Green's dyadic which can be expressed in terms of an angular spectrum of plane waves. In fact, for the far field it can be even more simplified by applying the method of stationary phase [15] to the two-dimensional angular integration. Using the abbreviation

$$g(\varphi,\vartheta) = k_i(\varphi,\vartheta)\ \cos\vartheta \tag{32}$$

the result reads

$$\begin{aligned}\underline{\underline{\mathcal{G}}}^a_{ee}(r,\phi,\theta) \cong \sum_{\substack{\text{outward trav.}\\ \text{waves i}}} \frac{-\sigma}{2\pi\sqrt{|ab-c^2|}}\,\underline{\underline{\mathbf{A}}}_i(\varphi_s,\vartheta_s)&\\ \times \sin\vartheta_s\ \frac{1}{r}\mathrm{e}^{-jk_i(\varphi_s,\vartheta_s)r\cos\vartheta_s} + \underline{\underline{\mathcal{I}}}_B&\end{aligned} \tag{33}$$

where

$$\sigma = \begin{cases} 1 & ;\ ab > c^2,\ a<0 \\ -1 & ;\ ab > c^2,\ a>0 \\ j & ;\ ab < c^2 \end{cases} \tag{34}$$

$$ab = \left[\frac{\partial^2 g}{\partial\varphi^2}\frac{\partial^2 g}{\partial\vartheta^2}\right]_{(\varphi_s,\vartheta_s)} \tag{35}$$

$$c = \left.\frac{\partial^2 g}{\partial\varphi\partial\vartheta}\right|_{(\varphi_s,\vartheta_s)} \tag{36}$$

The stationary phase angles (φ_s,ϑ_s) are determined by the condition

$$\left.\frac{\partial g}{\partial\varphi}\right|_{(\varphi_s,\vartheta_s)} = 0,\ \left.\frac{\partial g}{\partial\vartheta}\right|_{(\varphi_s,\vartheta_s)} = 0 \tag{37}$$

which corresponds to that point of the wavenumber surface obeying a normal vector parallel to $\mathbf{r}$. This result is not surprising in view of the fact, that this means that the group velocity at the stationary point is oriented in the direction of the observation point. We note that, e.g., for wavenumber surfaces featuring local 'valleys', more than one point could fulfill this condition. In this case, one has to sum up the contributions from all stationary points. The term $\underline{\underline{\mathcal{I}}}_B$ stands for additional asymptotic terms arising from contributions at the boundary of the integration range (see Appendix C). The radiating contribution, however, is given by the stationary phase expression as will be discussed below. In the above representation it was assumed that the stationary point is lying within the integration interval. For the special case that a stationary point lies on the integration boundary, the above result must be modified. For example in case of isotropic media, we have $\vartheta_s = 0$, which moreover yields a vanishing integrand at the stationary phase point due to the $\sin\vartheta$ term stemming from the Jacobian. Alternatively the stationary phase approximation can be evaluated in any other co-ordinate frame in a similar way, which then yields stationary points within the integration range, only.

Next let us consider the transformation related to the last term in (20). We label the corresponding part using the superscript d referring to the involved dyadic $\underline{\underline{\mathbf{D}}}$:

$$\underline{\underline{\mathcal{G}}}^d_{ee}(r,\phi,\theta) = \frac{1}{(2\pi)^3} \int_0^\pi d\vartheta \sin\vartheta \int_0^\pi d\varphi \int_{-\infty}^{\infty} dk \ \underline{\underline{\mathbf{D}}}(\varphi,\vartheta) \ k^2 \ \mathrm{e}^{-jkr\cos\vartheta} \tag{38}$$

Note that we again used different integration ranges for k, φ and ϑ. The k-integration can be formally performed recalling the identity

$$\int_{-\infty}^{\infty} dk \ \mathrm{e}^{-jka} = 2\pi\delta(a) \tag{39}$$

for the delta function. Further identities can be derived by differentiating the above expression with respect to a. We note that the formal justification for the application of the delta distribution can be obtained by considering the definition of the infinite range integration as limit $\int_{-\infty}^{+\infty} = \lim_{\alpha\to\infty} \int_{-\alpha}^{+\alpha}$ and noting that the function obtained after the finite range integration represents the δ distribution in the limit

$\alpha \to \infty$. Accordingly, the application of the integral representations for the derivatives of the delta function can be justified as well.

This leads to the following expression for $\underline{\underline{\mathcal{G}}}_{ee}^{d}$:

$$\underline{\underline{\mathcal{G}}}_{ee}^{d}(r,\phi,\theta) = \frac{-1}{(2\pi)^2} \int_0^{\pi} d\varphi \int_0^{\pi} d\vartheta \sin\vartheta \; \underline{\underline{\mathbf{D}}}(\varphi,\vartheta) \; \delta''(r\cos\vartheta) \tag{40}$$

where δ'' denotes the second derivative of the delta function with respect to its argument. The delta function indicates that the remaining two integrations can be further reduced to a single integration. Using [11]

$$\int_0^{\pi} d\vartheta \; \delta''(r\cos\vartheta) \; f(\vartheta) = \frac{f''(\pi/2) + f(\pi/2)}{r^3} \tag{41}$$

we obtain

$$\underline{\underline{\mathcal{G}}}_{ee}^{d}(r,\phi,\theta) = \frac{-1}{(2\pi)^2} \, \frac{1}{r^3} \int_0^{\pi} d\varphi \; \underline{\underline{\mathbf{D}}}_{\vartheta\vartheta}(\varphi,\pi/2) \tag{42a}$$

where $\underline{\underline{\mathbf{D}}}_{\vartheta\vartheta}$ denotes the second partial derivative of $\underline{\underline{\mathbf{D}}}$ with respect to ϑ. This gives contributions proportional to $1/r^3$. The remaining integration in φ constitutes a definite integral of a rational function in $\cos\varphi$ and $\sin\varphi$. By substituting $\exp j\varphi = \rho$, the integrand can be cast in a rational function in a complex variable ρ. Using symmetries of the integrands with respect to φ, the integral can be rewritten as an integral over the range $(0, 2\pi)$ which corresponds to an integration along the unit circle $|\rho| = 1$ in the complex ρ-plane. Using Cauchy's theorem, the integration can then be performed by determining all residues belonging to singularities of the integrand within the unit circle. For special cases, this integration can be principally done in closed form. However, in general, numerical integration can be performed with moderate computational effort, anyway.

The contributions related to dyadics $\underline{\underline{\mathbf{C}}}$ and $\underline{\underline{\mathbf{B}}}$ in (20) can be treated in a similar manner as shown above yielding contributions proportional to $1/r^2$ and $1/r$:

$$\underline{\underline{\mathcal{G}}}_{ee}^{c}(r,\phi,\theta) = \frac{j}{(2\pi)^2} \, \frac{1}{r^2} \int_0^{\pi} d\varphi \; \underline{\underline{\mathbf{C}}}_{\vartheta}(\varphi,\pi/2) \tag{42b}$$

$$\underline{\underline{\mathcal{G}}}_{ee}^{b}(r,\phi,\theta) = \frac{1}{(2\pi)^2}\,\frac{1}{r}\int\limits_0^{\pi} d\varphi\;\underline{\underline{\mathbf{B}}}(\varphi,\pi/2) \tag{42c}$$

such that the complete solution reads

$$\underline{\underline{\mathcal{G}}}_{ee}(r,\phi,\theta) = \underline{\underline{\mathcal{G}}}_{ee}^{a}(r,\phi,\theta) + \underline{\underline{\mathcal{G}}}_{ee}^{b}(r,\phi,\theta) + \underline{\underline{\mathcal{G}}}_{ee}^{c}(r,\phi,\theta) + \underline{\underline{\mathcal{G}}}_{ee}^{d}(r,\phi,\theta) \tag{43}$$

Here we used

$$\int\limits_0^{\pi} d\vartheta\;\delta^{(n)}(r\cos\vartheta)\;f(\vartheta) = \frac{f^{(n)}(\pi/2)}{r^{n+1}} \quad \text{for } n=0,1 \tag{44}$$

to perform the ϑ integrations, where the superscript (n) denotes the nth derivative. It is important to note, that equations (42) are exact representations involving no asymptotic approximation. In the limit $r \to 0$ the term $\underline{\underline{\mathcal{G}}}_{ee}^{a}$ in (43) can be neglected and the remaining terms describe the field behavior close to the dipole source. In the limit $r \to \infty$ we have the stationary phase expression being proportional to $\exp(-jk_{i,s}\cos\vartheta_s r)/r$ together with the additional term $\underline{\underline{\mathcal{I}}}_{B}$ as given in (33) plus additional contributions from $\underline{\underline{\mathcal{G}}}_{ee}^{b}, \underline{\underline{\mathcal{G}}}_{ee}^{c}$ and $\underline{\underline{\mathcal{G}}}_{ee}^{d}$ which are proportional to $1/r,\ 1/r^2$ and $1/r^3$, respectively. Of special interest is $\underline{\underline{\mathcal{G}}}_{ee}^{b}$ as it has the same $1/r$ behavior as the stationary phase expression except from the exponential $\exp(-jk_{i,s}\cos\vartheta_s r)$ being characteristic for propagating waves. From physical reasoning, a $1/r$ dependence without a 'wave-exponential' is not expected in the far field. However, by examining simple examples it turns out, that the 'non-physical' $1/r$ contributions from $\underline{\underline{\mathcal{G}}}_{ee}^{b}$ are asymptotically canceled by corresponding terms in $\underline{\underline{\mathcal{I}}}_{B}$. The fact that $\underline{\underline{\mathcal{I}}}_{B}$ actually shows $1/r$ behavior for $r \to \infty$ is discussed in Appendix C. Thus, as expected, the stationary phase expression alone yields the physical far field behavior.

3. Green's Dyadic for Diagonally Bianisotropic Media

Simple expressions can be achieved if, for instance, the solutions for the dispersion surfaces can be obtained in closed form. The polynomial $F(k_x,k_y,k_y,\omega)$ is of fourth order in the wavenumber components. This means that if, for instance, two wavenumber components of a plane wave are prescribed at a given frequency, the remaining component can be determined as the roots of a polynomial of fourth degree. This will yield four solutions which can, e.g., represent points on two closed wavenumber surfaces. Alternatively, the radial wavenumber coordinate k can be expressed in terms of the spherical angles for each wavenumber surface. Algebraic equations of fourth order can be solved principally in closed form, which, however, leads to fairly unwieldy expressions. In order to demonstrate the approach described before, we shall restrict to a class of media with diagonal bianisotropy. This means that we assume that the principal axes for each material tensor lie in real space and coincide (one may think of a bianisotropic crystal). The respective material parameter tensors in rectangular co-ordinates read

$$\begin{aligned} \underline{\underline{\varepsilon}} &= \begin{bmatrix} \varepsilon_1 & 0 & 0 \\ 0 & \varepsilon_2 & 0 \\ 0 & 0 & \varepsilon_3 \end{bmatrix}, \qquad \underline{\underline{\mu}} = \begin{bmatrix} \mu_1 & 0 & 0 \\ 0 & \mu_2 & 0 \\ 0 & 0 & \mu_3 \end{bmatrix} \\ \underline{\underline{\xi}} &= \begin{bmatrix} \xi_1 & 0 & 0 \\ 0 & \xi_2 & 0 \\ 0 & 0 & \xi_3 \end{bmatrix}, \qquad \underline{\underline{\zeta}} = \begin{bmatrix} \zeta_1 & 0 & 0 \\ 0 & \zeta_2 & 0 \\ 0 & 0 & \zeta_3 \end{bmatrix} \end{aligned} \tag{45}$$

The dispersion relation assumes the form

$$\begin{aligned} G(s_x, s_y, s_z) = {} & a_{11} s_x^4 + a_{22} s_y^4 + a_{33} s_z^4 + 2a_{12} s_x^2 s_y^2 + 2a_{23} s_y^2 s_z^2 + 2a_{31} s_z^2 s_x^2 \\ & + 2a_{14} s_x^2 + 2a_{24} s_y^2 + 2a_{34} s_z^2 + a_{44} + \gamma s_x s_y s_z = 0 \end{aligned} \tag{46}$$

where we used slownesses $s_\nu = k_\nu/\omega \ (\nu = x, y, z)$ to omit explicit frequency dependence. The expressions for the coefficients a_{ij} are listed in Appendix D while the coefficient γ is given below. The relation between $G(s_x, s_y, s_z)$ and $F(k_x, k_y, k_y, \omega)$ (see Eq. (8)) is given by

$$F(k_x, k_y, k_y, \omega) = -\frac{\omega^6}{\mu_1 \mu_2 \mu_3} \, G\left(\frac{k_x}{\omega}, \frac{k_y}{\omega}, \frac{k_z}{\omega}\right) \tag{47}$$

Obviously $G(s_x, s_y, s_z)$ is biquadratic in the slowness components apart from the term proportional to $s_x s_y s_z$ whose coefficient is given by

$$\gamma = -\sum_{k,l,m=\{1,2,3\}} \epsilon_{klm} \, \varepsilon_k \, \mu_l \, (\xi_m + \zeta_m) \tag{48}$$

where the sum runs over all possible permutations of $\{1, 2, 3\}$ and the Levi-Civita tensor is given by $\epsilon_{klm} = \pm 1$ if $\{k, l, m\}$ is an

$\begin{smallmatrix}\text{even}\\ \text{odd}\end{smallmatrix}$ permutation of $\{1,2,3\}$. If this coefficient vanishes, we are faced with a biquadratic dispersion relation. For instance this is the case for reciprocal media with $\xi_i = -\zeta_i$ or for media where

$$\frac{\varepsilon_l}{\varepsilon_m} = \frac{\mu_l}{\mu_m} = \frac{\xi_l + \zeta_l}{\xi_m + \zeta_m} \text{ with } l \neq m \text{ and } l, m \in \{1,2,3\} \tag{49}$$

to name two examples. Note that uniaxial media are a special case of the latter example. For the following let us assume that (48) vanishes. Introducing spherical co-ordinates k, α, β (not to be confused with the spherical co-ordinates k, φ, ϑ in the rotated frame) by setting

$$k_x = k\cos\alpha\sin\beta,\ k_y = k\sin\alpha\sin\beta,\ k_z = k\cos\beta \tag{50}$$

we can determine the wavenumber surface by solving a quadratic equation in k^2 for given α and β:

$$\frac{k_{1,2,3,4}}{\omega} = \pm\sqrt{\frac{-b \pm \sqrt{b^2 - 4ac}}{2a}} \tag{51}$$

where

$$\begin{aligned} a =&a_{33}\cos^4\beta + 2a_{31}\cos^2\alpha\cos^2\beta\sin^2\beta + 2a_{23}\cos^2\beta\sin^2\alpha\sin^2\beta \\ &+ a_{11}\cos^4\alpha\sin^4\beta + 2a_{12}\cos^2\alpha\sin^2\alpha\sin^4\beta + a_{22}\sin^4\alpha\sin^4\beta \end{aligned} \tag{52}$$

$$b = 2a_{34}\cos^2\beta + 2a_{14}\cos^2\alpha\sin^2\beta + 2a_{24}\sin^2\alpha\sin^2\beta \tag{53}$$

$$c = a_{44} \tag{54}$$

The four solutions $k_{1,2,3,4}$ are obtained by evaluating (51) for all possible combinations of the $\pm$ signs.

Thus the denominator F of spectral Green's dyadic can be written in factorized form. The numerator is essentially determined by $\underline{\underline{\widetilde{\mathcal{H}}}}^{adj}$, which is given in Appendix D.

As a numerical example let us consider a reciprocal medium with

$$\begin{aligned} &\underline{\underline{\varepsilon}} = \varepsilon_0 \begin{bmatrix} 1 & 0 & 0 \\ 0 & 1.2 & 0 \\ 0 & 0 & 1.7 \end{bmatrix}, \qquad \underline{\underline{\mu}} = \mu_0 \begin{bmatrix} 2 & 0 & 0 \\ 0 & 2.1 & 0 \\ 0 & 0 & 2.3 \end{bmatrix} \\ &\underline{\underline{\xi}} = j\sqrt{\mu_0\varepsilon_0} \begin{bmatrix} 0.3 & 0 & 0 \\ 0 & 0.2 & 0 \\ 0 & 0 & 0.31 \end{bmatrix}, \qquad \underline{\underline{\zeta}} = -\underline{\underline{\xi}} \end{aligned} \tag{55}$$

The wavenumber surfaces of this medium are shown in Figs. 4 (faster mode) and 6 (slower mode). The terms 'fast' and 'slow' here refer to the phase velocity ω/k which is larger for the faster mode. According to (33) the far field asymptotics consist of plane wave contributions related to each of these two modes:

$$\underline{\underline{\mathcal{G}}}_{ee} \cong \sum_{l=1}^{2} \underline{\underline{\mathcal{A}}}_l \, \frac{1}{r} \, \mathrm{e}^{-jk_i(\varphi_s,\vartheta_s) r \cos\vartheta_s} \tag{56}$$

where we introduced the abbreviation $\underline{\underline{\mathcal{A}}}_l$ (not to be confused with the dyadic $\underline{\underline{\mathbf{A}}}_i$) for the amplitudes appearing in (33) and the indices 1 and 2 refer to the faster and the slower mode, respectively. We calculated the asymptotics for a z oriented dipole $J_z = I_0 d \ \delta(\mathbf{r})$, hence the electric fields correspond to the column $\mathcal{G}_{ee,i3}$ $(i = 1, 2, 3)$ of Green's dyadic. We show plots for the θ component of the electric field given by

$$\frac{E_\theta}{I_0 d} = -\mathcal{G}_{ee,33} \sin\theta + \mathcal{G}_{ee,23} \cos\theta \sin\phi + \mathcal{G}_{ee,13} \cos\theta \cos\phi \tag{57}$$

leading to a corresponding definition for the related modal amplitudes $\underline{\underline{\mathcal{A}}}_l$:

$$\mathcal{A}_{\theta,l} = -\mathcal{A}_{33,l} \sin\theta + \mathcal{A}_{23,l} \cos\theta \sin\phi + \mathcal{A}_{13,l} \cos\theta \cos\phi \tag{58}$$

Figure 5 shows a 3D polar plot of the far field amplitude

$$\frac{2\pi}{\omega\mu_0} |\mathcal{A}_{\theta,l}| \tag{59}$$

related to faster mode ($l = 1$) and Fig. 7 shows the respective amplitude for the slower mode ($l = 2$).

Finally, Fig. 8 shows a 3D polar plot of the amplitude

$$8\pi^2 \omega\varepsilon_0 \lim_{r\to 0} \left| r^3 \frac{E_\theta}{I_0 d} \right| \tag{60}$$

describing the singular behavior close to the source which has been calculated by evaluating $\underline{\underline{\mathcal{G}}}^d_{ee}$.

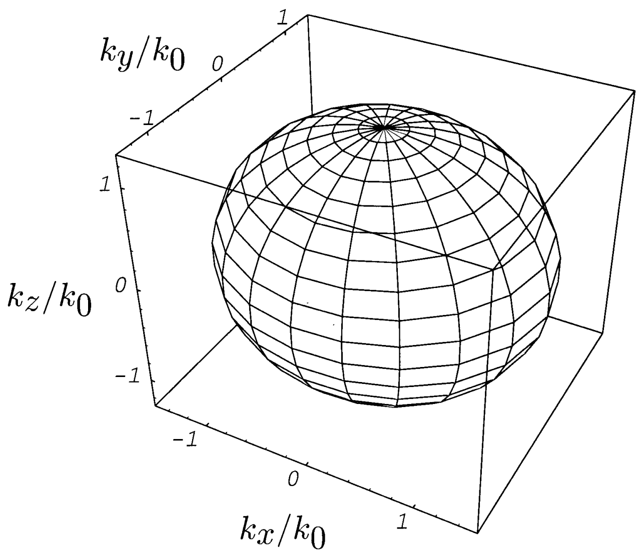

Figure 4. Wavenumber surface of the faster mode (k_0 = free-space wavenumber).

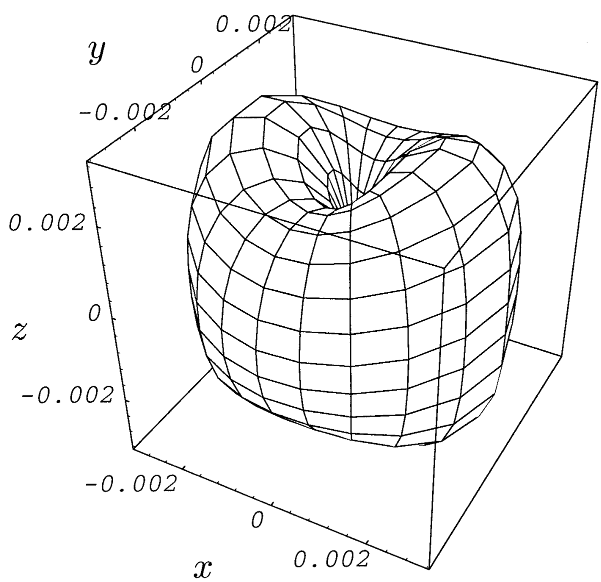

Figure 5. Far field amplitude of waves related to faster mode (3D polar plot, see (59) for axes scaling).

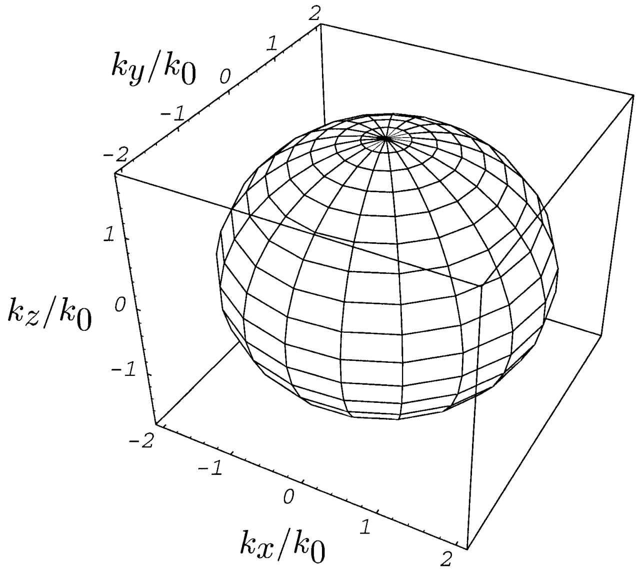

Figure 6. Wavenumber surface of the slower mode (k_0 = free-space wavenumber).

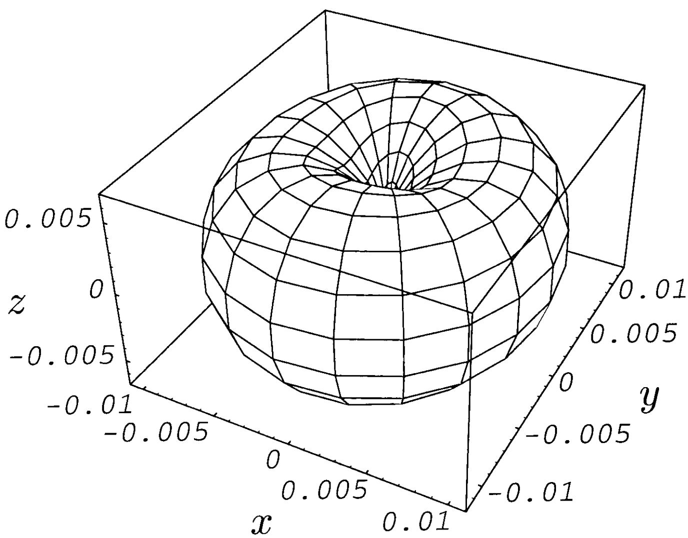

Figure 7. Far field amplitude of waves related to slower mode (3D polar plot, see (59) for axes scaling).

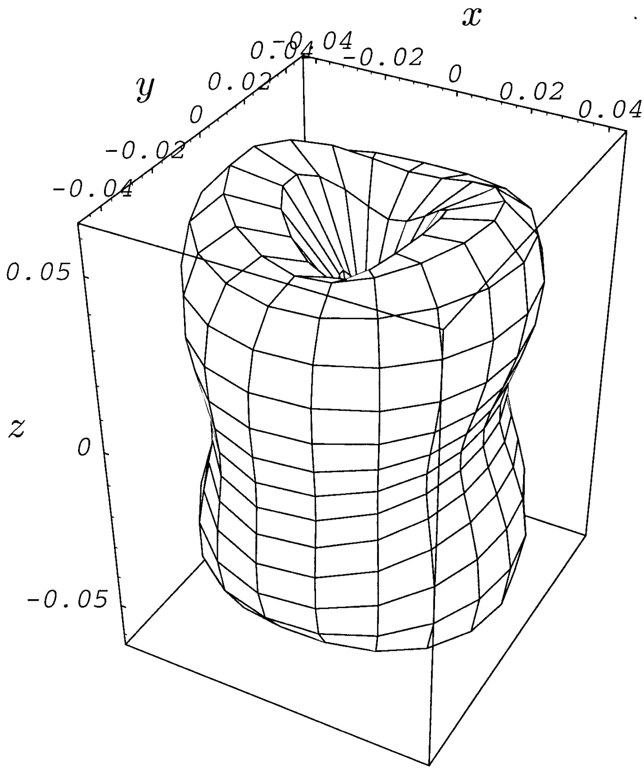

Figure 8. Coefficient for the $1/r^3$ singularity (3D polar plot, see (60) for axes scaling).

4. Conclusion

A method for the derivation for the far- as well as the near-field asymptotic expressions for Green's dyadics in infinitely extended, bianisotropic media has been presented. The involved decomposition in spectral domain has been discussed and formulae for the spatial domain representations of the resulting partial terms have been derived. To show the applicability of the method, explicit expressions for diagonally bianisotropic media have been provided together with numerical examples.

Appendix A: The Rotated Co-ordinate Frame.

Using the approach leading to (13), the coefficient dyadics $\underline{\underline{\mathbf{A}}}$, $\underline{\underline{\mathbf{B}}}$, $\underline{\underline{\mathbf{C}}}$ and $\underline{\underline{\mathbf{D}}}$ can be easily determined from spectral Green's dyadic as a rational function in the normalized rectangular wavenumber components k_i/k (with $k = \sqrt{k_x^2 + k_y^2 + k_z^2}$). The wavenumber vector $[k_x, k_y, k_z]^T$ in the original frame transforms as follows into the rotated frame (see Fig. 1):

$$\begin{bmatrix} k_{x'} \\ k_{y'} \\ k_{z'} \end{bmatrix} = \underline{\underline{\mathbf{T}}}(\phi, \theta) \cdot \begin{bmatrix} k_x \\ k_y \\ k_z \end{bmatrix} \tag{61}$$

where the transformation matrix reads

$$\underline{\underline{\mathbf{T}}}(\phi, \theta) = \begin{bmatrix} \sin\phi & -\cos\phi & 0 \\ \cos\theta\cos\phi & \cos\theta\sin\phi & -\sin\theta \\ \sin\theta\cos\phi & \sin\theta\sin\phi & \cos\theta \end{bmatrix} \tag{62}$$

and primed quantities refer to rectangular components in the rotated frame. As the euclidian length $k = k'$ is invariant with respect to this transform, the normalized wavenumber components k_ν/k $(\nu = x, y, z)$ transform in the same manner. Introducing spherical co-ordinates

$$k_{x'} = k\sin\vartheta\cos\varphi, \;\; k_{y'} = k\sin\vartheta\sin\varphi, \;\; k_{z'} = k\cos\vartheta \tag{63}$$

we then arrive at the following substitution rule for the normalized rectangular wavenumber components:

$$\frac{1}{k}\begin{bmatrix} k_x \\ k_y \\ k_z \end{bmatrix} = \underline{\underline{\mathbf{T}}}^{-1} \cdot \begin{bmatrix} \sin\vartheta\cos\varphi \\ \sin\vartheta\sin\varphi \\ \cos\vartheta \end{bmatrix} = \underline{\underline{\mathbf{T}}}^{T} \cdot \begin{bmatrix} \sin\vartheta\cos\varphi \\ \sin\vartheta\sin\varphi \\ \cos\vartheta \end{bmatrix} \tag{64}$$

As we are dealing with a simple rotation of the co-ordinate system, the inverse of the transformation matrix is given by its transpose: $\underline{\underline{\mathbf{T}}}^{-1} = \underline{\underline{\mathbf{T}}}^{T}$.

Appendix B: Double Roots in the Dispersion Equation.

A double zero means that for a given direction (φ, ϑ) two of the four solutions of the dispersion equation coincide. If we label the associated wavenumber k_s, this means that the eigenvalue problem associated with the matrix $\underline{\underline{\widetilde{\mathcal{H}}}}(k,\varphi,\vartheta)$

$$\underline{\underline{\widetilde{\mathcal{H}}}} \cdot \widetilde{\mathbf{E}}_i = \lambda_i \widetilde{\mathbf{E}}_i \tag{65}$$

yields two eigenvalues having a first order zero or one eigenvalue featuring a double zero at $k = k_s$. Eigenvectors corresponding to zero eigenvalues $\lambda_i = 0$ represent the electric field vectors associated with plane wave solutions. The crucial point is, that we can commonly always establish two linearly independent plane wave solutions which means that we must have two eigenvalues (say λ_1 and λ_2) with single zeros at $k = k_s$ related to linearly independent eigenvectors $\widetilde{\mathbf{E}}_1$ and $\widetilde{\mathbf{E}}_2$. For instance, in case of isotropic media these linearly independent eigenvectors represent different polarizations of the corresponding plane waves. The third eigenvector $\widetilde{\mathbf{E}}_3$ related to the eigenvalue $\lambda_3 \neq 0$, is always linearly independent of the other eigenvectors. Hence the matrix set up by the eigenvectors

$$\underline{\underline{\mathbf{E}}} = [\widetilde{\mathbf{E}}_1, \widetilde{\mathbf{E}}_2, \widetilde{\mathbf{E}}_3] \tag{66}$$

is not singular at $k = k_s$ and the decomposition

$$\underline{\underline{\widetilde{\mathcal{H}}}} = \underline{\underline{\mathbf{E}}} \cdot \begin{bmatrix} \lambda_1 & 0 & 0 \\ 0 & \lambda_2 & 0 \\ 0 & 0 & \lambda_3 \end{bmatrix} \cdot \underline{\underline{\mathbf{E}}}^{-1}, \tag{67}$$

exists even if two eigenvalues equal zero. Accordingly, Green's dyadic can be written as

$$\underline{\underline{\widetilde{\mathcal{G}}}}_{ee} = -j\omega \underline{\underline{\mathbf{E}}} \cdot \begin{bmatrix} \frac{1}{\lambda_1} & 0 & 0 \\ 0 & \frac{1}{\lambda_2} & 0 \\ 0 & 0 & \frac{1}{\lambda_3} \end{bmatrix} \cdot \underline{\underline{\mathbf{E}}}^{-1} \tag{68}$$

Since λ_1 and λ_2 show a first order zero at k_s, the Green's dyadic shows a first order pole at k_s.

Appendix C: Asymptotic Contributions from the Boundary of the Integration Range.

We are faced with the asymptotic evaluation of integrals of the type

$$\int_0^{2\pi} d\varphi \int_0^{\pi/2} d\vartheta \ \sin\vartheta \ \underline{\underline{\mathbf{A}}}_i(\varphi,\vartheta) \ \mathrm{e}^{-jk_i(\varphi,\vartheta)r\cos\vartheta} \tag{69}$$

in the limit $r \to \infty$. The integrand is highly oscillatory except at stationary phase points. Apart from contributions from the stationary phase points, which can be treated in the standard fashion [15], it is well known that for integrals with oscillatory integrands and a finite integration range, additional asymptotic contributions arise from the end points of the integration range. Commonly, these contributions show higher decay towards infinity as the stationary phase expression and can thus be neglected. For instance, for one dimensional integrations the envelope of the stationary phase term is proportional to $1/\sqrt{r}$ while the boundary contributions have envelopes proportional to $1/r$ [9]. In case of our double integration the behavior is somewhat different which essentially is related to the fact that the integrand does not oscillate along the boundary line $\vartheta = \pi/2$. A rigorous mathematical treatment of asymptotic endpoint contributions can be found in [16]. In the following we provide a brief heuristic consideration adapted to our case. Let us deal with the endpoint $\pi/2$ of the ϑ integration first. In the vicinity of $\vartheta = \pi/2$ the integrand can be approximated as

$$\underline{\underline{\mathbf{A}}}_i(\varphi,\pi/2) \ \mathrm{e}^{+jk_i(\varphi,\pi/2) \ (\vartheta-\pi/2) \ r} \tag{70}$$

Hence the end point contribution of the ϑ integration can be asymptotically approximated by

$$\lim_{\delta\to 0+} \int_{-\infty}^{\pi/2} d\vartheta \ \underline{\underline{\mathbf{A}}}_i(\varphi,\pi/2) \ \mathrm{e}^{jk_i(\varphi,\pi/2) \ (\vartheta-\pi/2) \ r} \ \mathrm{e}^{\delta\vartheta} = \frac{\underline{\underline{\mathbf{A}}}_i(\varphi,\pi/2)}{jk_i(\varphi,\pi/2)} \ \frac{1}{r} \tag{71}$$

where the vanishingly small positive quantity δ has been introduced to ensure convergence of the integral at $-\infty$ (one might alternatively think of introducing vanishingly small losses leading to an appropriate imaginary part of k_i). Obviously, $\delta \to 0$ does not influence the behavior at the integrand in the vicinity of $\vartheta = \pi/2$. In a similar manner it can be shown, that the second end point contribution yields contributions with envelopes decaying faster than $1/r$ except for the special case $k_{i,\vartheta}(\phi, 0) = 0$, which, however, means that the endpoint is a stationary point and thus part of the stationary phase contribution.

With the remaining φ integration the asymptotic end point contribution $\underline{\underline{\mathcal{I}}}_B$ in (33) can thus be written as

$$\underline{\underline{\mathcal{I}}}_B = -\frac{1}{(2\pi)^2}\,\frac{1}{r}\int_0^{2\pi} d\varphi \sum_{\substack{\text{outward trav.}\\ \text{waves}}} \frac{\underline{\underline{\mathbf{A}}}_i(\varphi, \pi/2)}{k_i(\varphi, \pi/2)} \tag{72}$$

showing the $1/r$ dependence of $\underline{\underline{\mathcal{I}}}_B$.

Appendix D: Explicit Forms of a_{ij} and $\underline{\underline{\widetilde{\mathcal{H}}}}^{adj}$.

The coefficients a_{ij} in (46) are given by

$$2a_{ij} = \varepsilon_j\mu_i + \varepsilon_i\mu_j - \xi_j\zeta_i - \xi_i\zeta_j (\text{for } \; i, j = 1, 2, 3) \tag{73}$$

$$2a_{14} = -a_{11}\;(\varepsilon_3\mu_2 + \varepsilon_2\mu_3 - \xi_2\xi_3 - \zeta_2\zeta_3) \tag{74}$$

$$2a_{24} = -a_{22}\;(\varepsilon_3\mu_1 + \varepsilon_1\mu_3 - \xi_1\xi_3 - \zeta_1\zeta_3) \tag{75}$$

$$2a_{34} = -a_{33}(\varepsilon_2\mu_1 + \varepsilon_1\mu_2 - \xi_1\xi_2 - \zeta_1\zeta_2) \tag{76}$$

$$a_{44} = a_{11}\;a_{22}\;a_{33} \tag{77}$$

It is sufficient to provide the Green's functions $\mathcal{G}_{ee,i3}$ with $i = 1, 2, 3$ since the other elements of the Green's dyadic can be obtained by applying appropriate symmetry transforms [10]. In terms of slownesses we have the following expressions for the adjoint matrix (see (14))

$$\begin{aligned}\widetilde{\mathcal{H}}_{13}^{adj} =& \frac{\omega^4}{\mu_1\mu_2\mu_3}\Big\{\mu_1 s_x^3 s_z + s_x^2 s_y(\mu_2\xi_1 - \mu_1\xi_2) + s_y\,[-\varepsilon_2\mu_2\mu_3\xi_1 \\ &+\mu_3\xi_1\xi_2\zeta_2 + \varepsilon_2\mu_1\mu_2\zeta_3 - \mu_1\xi_2\zeta_2\zeta_3 + s_z^2(\mu_3\zeta_2 - \mu_2\zeta_3)\,] \\ &+ s_x\,[\mu_2 s_y^2 s_z + \mu_3 s_z^3 + s_z(-\varepsilon_2\mu_1\mu_3 + \mu_3\xi_1\xi_2 - \mu_2\xi_1\zeta_3 + \mu_1\zeta_2\zeta_3)\,]\Big\}\end{aligned} \tag{78}$$

$$
\begin{aligned}
\widetilde{\mathcal{H}}_{23}^{adj} =& \frac{\omega^4}{\mu_1\mu_2\mu_3}\Big\{\mu_1 s_x^2 s_y s_z + \mu_2 s_y^3 s_z + s_x\left[\varepsilon_1\mu_1\mu_3\xi_2 + s_y^2(\mu_2\xi_1 - \mu_1\xi_2)\right.\\
&-\mu_3\xi_1\xi_2\zeta_1 - \varepsilon_1\mu_1\mu_2\zeta_3 + \mu_2\xi_1\zeta_1\zeta_3 + s_z^2(-\mu_3\zeta_1 + \mu_1\zeta_3)\left.\right]\\
&+s_y\left[\mu_3 s_z^3 + s_z(-\varepsilon_1\mu_2\mu_3 + \mu_3\xi_1\xi_2 - \mu_1\xi_2\zeta_3 + \mu_2\zeta_1\zeta_3)\right]\Big\} \qquad (79)
\end{aligned}
$$

$$
\begin{aligned}
\widetilde{\mathcal{H}}_{33}^{adj} =& \frac{\omega^4}{\mu_1\mu_2\mu_3}\Big\{\varepsilon_1\varepsilon_2\mu_1\mu_2\mu_3 + \mu_3 s_z^4 - \varepsilon_2\mu_2\mu_3\xi_1\zeta_1\\
&+ s_x^2(-\varepsilon_1\mu_1\mu_2 + \mu_1 s_z^2 + \mu_2\xi_1\zeta_1) - \varepsilon_1\mu_1\mu_3\xi_2\zeta_2 + \mu_3\xi_1\xi_2\zeta_1\zeta_2\\
&+ s_x s_y s_z(\mu_2\xi_1 - \mu_1\xi_2 + \mu_2\zeta_1 - \mu_1\zeta_2)\\
&+ s_y^2(-\varepsilon_2\mu_1\mu_2 + \mu_2 s_z^2 + \mu_1\xi_2\zeta_2)\\
&+ s_z^2(-\varepsilon_2\mu_1\mu_3 - \varepsilon_1\mu_2\mu_3 + \mu_3\xi_1\xi_2 + \mu_3\zeta_1\zeta_2)\Big\}. \qquad (80)
\end{aligned}
$$

With these expressions, the Green's dyadic can be obtained by considering Equations (13) and (14). The denominator polynomial has been given above (see Eqs. (46) and (47)). All expressions can be transformed into spherical co-ordinates in the rotated frame as it is shown in Appendix A.

Acknowledgments

The work of Bernhard Jakoby was supported by the Austrian Fonds zur Förderung der wissenschaftlichen Forschung (Erwin Schrödinger grant J00975-TEC). Frank Olyslager is a post-doctoral researcher of the Belgian National Fund for Scientific Research.

References

1. Mariotte, F., and J. P. Parneix, eds., *Proceedings of the CHIRAL'94* (Périgueux, France), May 1994.
2. Kong, J. A., *Electromagnetic Wave Theory*. New York, John Wiley & Sons, 2nd ed., 1990.
3. Lindell, I. V., and F. Olyslager, "Duality transformations, Green's dyadics and plane wave solutions for a class of bianisotropic media," *Journal of Electromagnetic Waves and Applications*, Vol. 9, 85–96, January 1995.

4. Olyslager, F., "Time-harmonic two- and three-dimensional Green's dyadics for general uniaxial bianisotropic media," *IEEE Trans. on Antennas Propagat.*, Vol. 43, No. 4, 430–434, 1995.
5. Weiglhofer, W. S., "Analytic methods and free-space dyadic Green's functions," *Radio Science*, Vol. 28, No. 5, 847–857, 1993.
6. Mittra, R., and G. A. Deschamps, "Field solution for a dipole in an anisotropic medium," in *Electromagnetic Theory and Antennas* (E. C. Jordan, ed.), 495–512, 1963.
7. Lindell, I. V., *Methods for Electromagnetic Field Analysis.* New York, Oxford University Press, 1992.
8. Collin, R. E., *Field Theory of Guided Waves.* New YorK, IEEE Press, 2nd ed., 1991.
9. Felsen, L. B., and N. Marcuvitz, *Radiation and Scattering of Waves.* Englewood Cliffs, New Jersey, Prentice-Hall, 1973.
10. Graglia, R. D., P. L. E. Uslenghi, and R. E. Zich, "Dispersion relations for bianisotropic materials and its symmetry properties," *IEEE Trans. on Antennas Propagat.*, Vol. 39, No. 1, 83–90, 1990.
11. Jakoby, B., *Analysis of Electromagnetic Fields in Stratified Complex Media.* Ph.D. thesis, Vienna University of Technology, 1994.
12. Van Bladel, J., *Electromagnetic Fields.* New York, McGraw-Hill, 1964.
13. Cottis, P. G., and G. D. Kondylis,"Properties of the dyadic Green's function for an unbounded anisotropic medium," *IEEE Trans. on Antennas Propagat.*, Vol. 43, 154–161, February 1995.
14. Okoshi, T., *Planar Circuits for Microwaves and Lightwaves.* Berlin-Heidelberg-New York: Springer Verlag, 1985.
15. Jull, E., *Aperture Antennas and Diffraction Theory*, Vol. 10 of *IEE Electromagnetic Wave Series.* Stevenage, UK, and New York, Peter Peregrinus Ltd., 1981.
16. Bleistein, N., and R. A. Handelsman, *Asymptotic Expansions of Integrals.* New York, Holt, Rinehart and Winston, 1975.